

Optimal target VOI size for accurate 4D coregistration of DCE-MRI

Brian Park^{*a}, Artem Mikheev^b, Youssef Zaim Wadghiri^b, Anne Bertrand^c, Dmitry Novikov^b, Hersh Chandarana^b, Henry Rusinek^b

^aDept. of Radiology, Hospital of the University of Pennsylvania, 3400 Spruce St., Philadelphia, PA USA 19104; ^bDept. of Radiology, NYU Langone Medical Center, 333 E 38th St., New York, NY USA 10016; ^cDept. of Functional and Diagnostic Neuroradiology, Pitié-Salpêtrière Hospital, 47-83 Boulevard de l'Hôpital, 75013 Paris, France.

ABSTRACT

Dynamic contrast enhanced (DCE) MRI has emerged as a reliable and diagnostically useful functional imaging technique. DCE protocol typically lasts 3-15 minutes and results in a time series of N volumes. For automated analysis, it is important that volumes acquired at different times be spatially coregistered. We have recently introduced a novel 4D, or volume time series, coregistration tool based on a user-specified target volume of interest (VOI). However, the relationship between coregistration accuracy and target VOI size has not been investigated. In this study, coregistration accuracy was quantitatively measured using various sized target VOIs. Coregistration of 10 DCE-MRI mouse head image sets were performed with various sized VOIs targeting the mouse brain. Accuracy was quantified by measures based on the union and standard deviation of the coregistered volume time series. Coregistration accuracy was determined to improve rapidly as the size of the VOI increased and approached the approximate volume of the target (mouse brain). Further inflation of the VOI beyond the volume of the target (mouse brain) only marginally improved coregistration accuracy. The CPU time needed to accomplish coregistration is a linear function of N that varied gradually with VOI size. From the results of this study, we recommend the optimal size of the VOI to be slightly overinclusive, approximately by 5 voxels, of the target for computationally efficient and accurate coregistration.

Keywords: volume of interest, VOI, target size, registration, registration accuracy, 4D, DCE-MRI, dynamic contrast-enhanced MRI

1. INTRODUCTION

A multitude of medical imaging coregistration algorithms have been developed, each with advantages for a specific application¹. Although a variety of options including different models, methods, and strategies can be selected and compared, the size of the target region is not commonly appreciated or emphasized. The target VOI size can have a significant impact on the accuracy and efficiency of a coregistration algorithm. In order to evaluate the size of the target region on coregistration accuracy, a reliable and robust measurement of coregistration accuracy needs to be identified.

DCE-MRI is a functional imaging technique consisting of a volume time series, or 4D data. Accurate coregistration is needed for automated quantitative functional analysis. However, there is still no validated measure for easy assessment of the accuracy of the alignment of N volumes. Intersection-based accuracy measures, such as the Dice similarity coefficient, have been widely accepted and used, but have intrinsic issues. These measures are non-linear and saturate quickly if one object in the series is completely misaligned. As a result, the overall degree of misalignment cannot be adequately ascertained since one perturbation may completely trump the alignment of the entire series. Additionally, the Dice similarity coefficient was originally derived for the ecologic association between two different species², which may not ideally extend to imaging data with greater than two series.

In this study, we propose new measures of coregistration accuracy based on the union and standard deviation of misaligned objects, and use these measures to compare the effect of target VOI size to coregistration accuracy of DCE-MRI mouse head images.

*brian.park@uphs.upenn.edu

2. METHODOLOGY

2.1 Simulation

New measures to assess registration accuracy based on union and standard deviation (defined below) of misaligned objects were validated through simulation of 100 cases consisting of groups of 10 line segments, each of which were randomly aligned. These were compared to the Dice similarity coefficient (DSC)²:

$$DSC(X, Y) = \frac{2|X \cap Y|}{|X| + |Y|} \quad (1)$$

where X and Y represent two samples, the numerator represents the intersection of the two samples, and the denominator represents the union of the two samples. A DSC of 1 indicates perfect alignment and 0 indicates no overlap. Simulations were performed using MATLAB and the linearity of each measure was evaluated using Pearson's coefficient.

2.2 DCE-MRI mouse head

Ten cases of C57Bl6 wild type mouse brains were used for analysis based on MRI protocol by Bertrand *et al*³. Briefly, a solution of MnCl₂ in saline (1.5μL of 5M MnCl₂) was administered under anesthesia (5% isoflurane) into one nostril of the mouse using a micropipette under microscopic control. The instillation led to manganese (Mn) uptake in the nasal epithelium. Mn then propagated along the olfactory tract to accumulate transiently in high concentration and to appear by its presence as a hyperintensity using a T1-weighted sequence. In each imaging time course, mice were scanned once prior to Mn administration followed by 8 repeated acquisitions over 7 days to generate 9 three-dimensional (3D) whole mouse head datasets. Each mouse head MRI dataset was acquired under 15 minutes using a 3D-T1 SPGR sequence (TR/TE/FA = 15ms/4ms/18°, 128×128×64 matrix, field of view = 19.2×19.2×9.6mm, averages = 6 leading to a 150μm isotropic resolution).

2.3 4D Coregistration

For 4D coregistration, let $i \in [1 \dots N]$ be the time index and $T_{i,j}$ the transformation that maps the coordinates of source volume i into the target volume j . T was restricted to a rigid body transform defined by its 3 translational and 3 rotational parameters, and computed to maximize signal cross-correlation between the target and the transformed source. Optimization was done in two stages: S1) an exhaustive search over a discrete grid of translational and rotational parameters distributed in the 6-dimensional parameter space; and S2) an iterative search for a local maximum of cross-correlation, initialized at the most promising grid points from stage S1. Coregistration was done using a radial algorithm with target g whereby all volumes were transformed to time point g by computing $T_{1,g}, T_{2,g}, T_{3,g} \dots$. The organ to be registered was specified interactively on a single time point (see Figure 1) using a target VOI. The initial target VOI (0 voxels inflation) was drawn manually by visual inspection to closely approximate the volume of the mouse brain. The morphology of this initial VOI was subsequently isotropically deflated/inflated in increments of 5 voxels to establish various sized target VOIs.

The coregistration software (FireVoxel) is written in C++ and uses Microsoft Foundation Class and Intel Threading Building Blocks libraries. The program features multi-core processor parallelism. All tests were performed on a desktop computer equipped with a Core i5-2400 3.10 GHz quad core processor. Data analysis was performed using MATLAB.

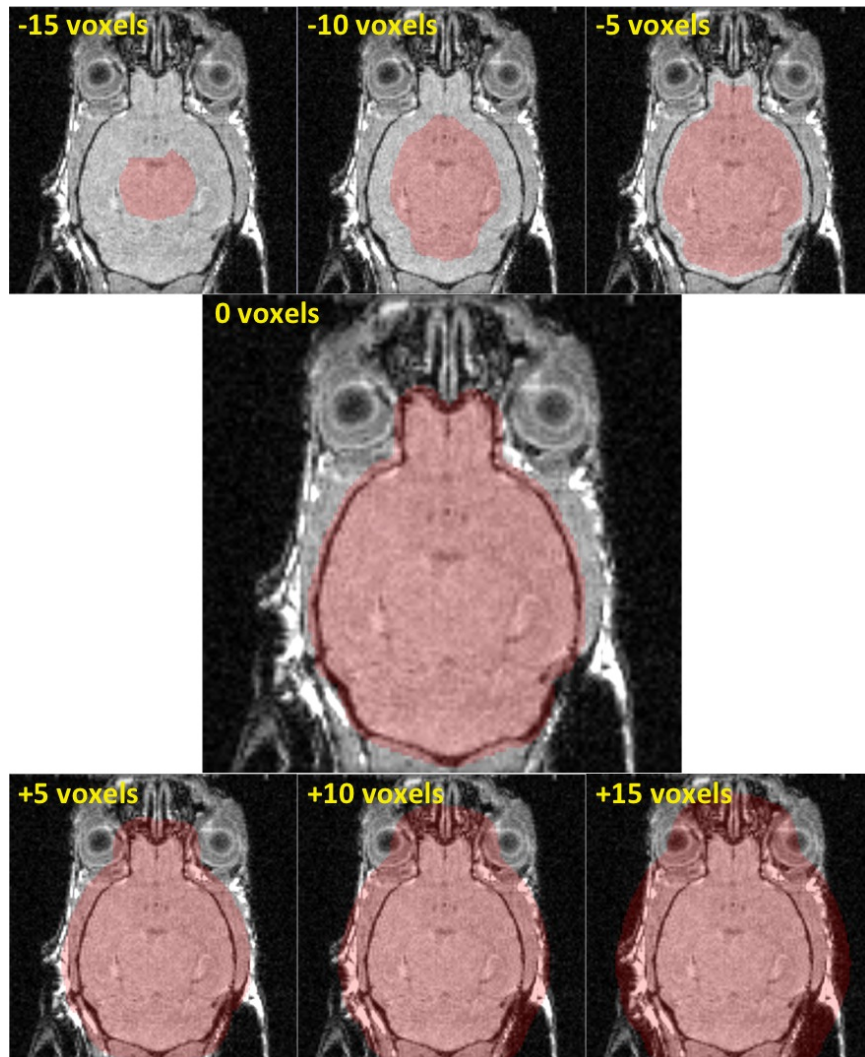


Figure 1. Various target VOIs of the mouse brain (T1-weighted MRI with 150 μ m isotropic resolution). Although the image and VOI are three-dimensional, only a single volume slice is shown for simplicity. Initial target VOI (0 voxels) closely approximates the volume of the mouse brain. Numbers in yellow represent isotropic deflation/inflation of the initial target VOI in increments of 5 voxels.

2.4 Registration accuracy

Registration accuracy can be quantified if the organ of interest is segmented at each time point. Let R_i be a 3D binary mask (1 = on, 0 = off) constructed from unregistered volumes at time i . Masks R_i were manually constructed by visualization and were not used for coregistration. Let $T_{i..}$ denote the optimal transformation constructed from coregistration. We construct transformed binary masks R'_i by voxel subsampling, application of $T_{i..}$, nearest-neighbor interpolation, and thresholding the results at a level > 0.5 . Two linear indices were used to quantify coregistration accuracy. We define index A (0 = perfect alignment and increasing values indicating greater misalignment) as the volume of the union of transformed masks R'_i subtracted by the ideal union (perfect alignment) represented by the maximum volume of a single untransformed mask R_i :

$$A = \text{union} - \text{ideal union} = \text{Vol} \bigcup_{i=1}^N R'_i - \max(\text{Vol} R_i) \quad (2)$$

We define index B (0 = perfect alignment and increasing values indicating greater misalignment) as the ideal standard deviation (perfect alignment) represented by the maximum standard deviation of a single untransformed mask R_i multiplied by N and subtracted by the standard deviation of the sum of the transformed masks R'_i :

$$B = \text{ideal stdev} - \text{stdev} = \max\left(\text{stdev}\left(N \times R_i\right)\right) - \text{stdev}\left(\sum_{i=1}^N R'_i\right) \quad (3)$$

3. RESULTS

3.1 New accuracy measures

New measures to assess coregistration accuracy based on union (index A) and standard deviation (index B) were validated using 100 cases of randomly aligned groups of 10 line segments (see Figure 2A). Intersection-based accuracy measures, such as the Dice similarity coefficient, are nonlinear and saturate quickly as the average misalignment d of each line segment increases (see Figure 2B). As a result, measures like the Dice similarity coefficient are volatile to single stray objects; one grossly misaligned object can bias the measure and exaggerate the overall misalignment of the group even if the remaining objects in the group are in near-perfect alignment.

In contrast to intersection-based measures, both union-based (index A) and standard deviation-based (index B) measures do not saturate and follow a strong linear relationship (see Figure 2C and D), where 0 represents perfect alignment and increasing values indicate a greater degree of overall misalignment. The negative sign in index B (see Equation 3) reflects the relationship of decreasing standard deviation with increasing misalignment (see Figure 3). With these measures, the overall alignment of the group is less influenced by single stray objects.

Both index A and index B demonstrated strong linear relationships with average misalignment. Index B was consistently found to have a stronger linear relationship, as determined by the greater Pearson's correlation coefficient, compared to index A based on 50 iterations of 100 cases of randomly aligned groups of 10 line segments (see Figure 2E). Therefore, index B is systemically more robust than index A and has a better correlation with misregistration.

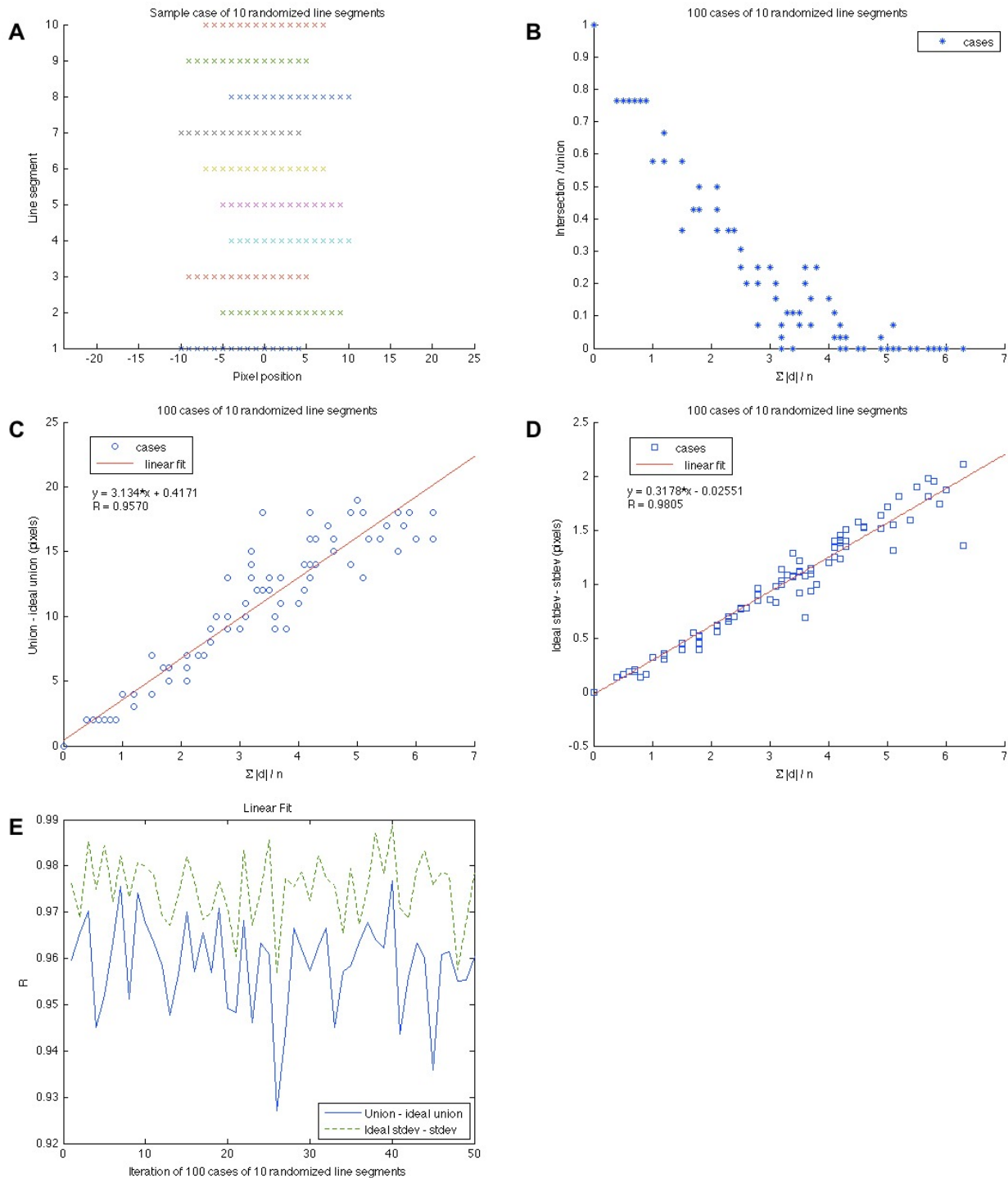


Figure 2. Simulations of line segments with random displacements d in position. A) One example case of misaligned line segments. B) Dice similarity coefficient (intersection divided by union) of 100 example cases to average displacement d of each case. C&D) Linear fit of 100 example cases to union (index A) and standard deviation (index B) measures to average displacement d of each case, respectively. E) Pearson's correlation coefficient (R) from linear fit of 50 iterations of 100 example cases.

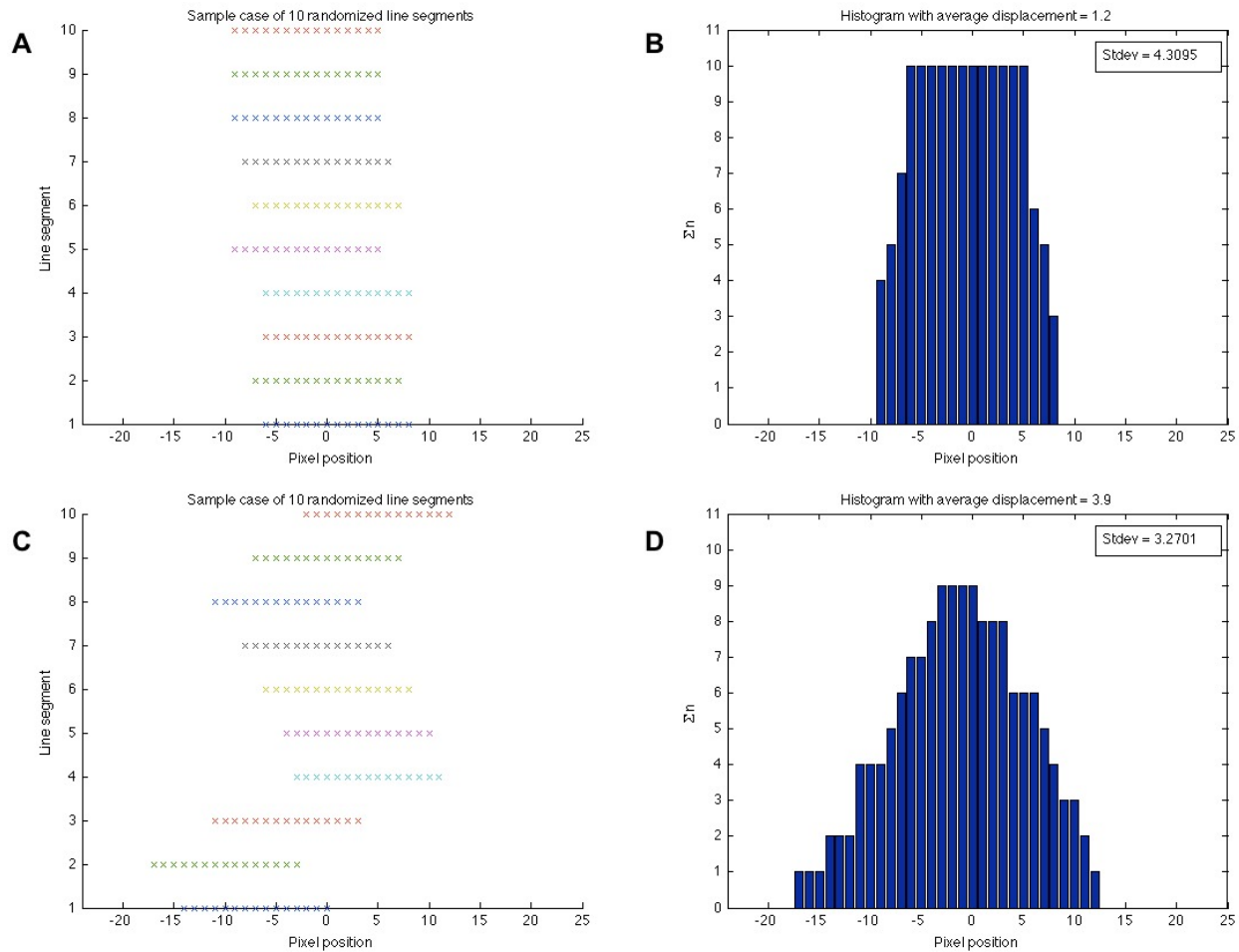


Figure 3. Sample cases demonstrating decreasing standard deviation with increasing misalignment. A) Example case of misaligned line segments with average displacement of 1.2 pixels. B) Histogram of A resulting in standard deviation of 4.3 pixels. C) Example case of misaligned line segments with increased average displacement of 3.9 pixels. D) Histogram of C resulting in standard deviation of 3.3 pixels.

3.2 Optimal target VOI size

The accuracy of coregistration based on union (index A) and standard deviation (index B) measures were found to rapidly improve with VOIs approaching the approximate volume of the mouse brain, or 0 voxels inflation. Further inflation of the VOI beyond 0 voxels displayed little to no improvement in coregistration accuracy (see Figure 4). Although both index A and index B were lowest, or had the greatest accuracy, with coregistration performed using a VOI with 5 voxels inflation, the improvement in accuracy was not statistically significant compared to 0 voxels or 10 voxels inflation.

The CPU time needed to accomplish coregistration is a linear function of N that was also found to increase linearly ($R = 0.99$) with target VOI size. For $N=9$, volume raster $128 \times 128 \times 64$, and similarity measure set to signal cross-correlation, the average CPU time ranged from 4.9 sec with -15 voxels inflation to 32.0 sec with 15 voxels inflation on a conventional workstation.

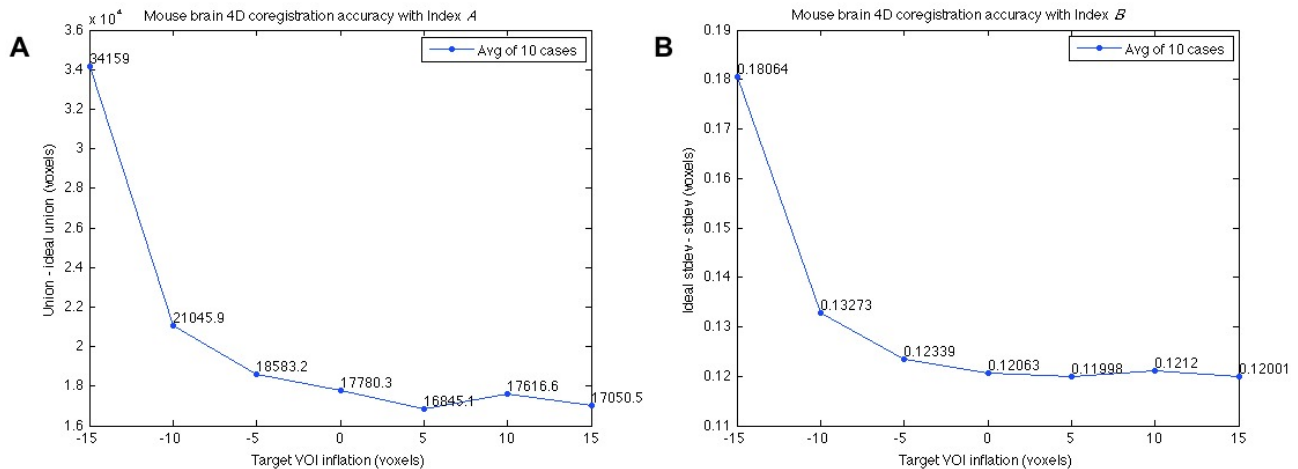


Figure 4. Relationship of registration accuracy versus target VOI size. Decreasing values of index *A* and index *B* indicate greater accuracy. A) Registration accuracy measured by index *A* with target VOI size. B) Registration accuracy measured by index *B* with target VOI size. Both index *A* and index *B* rapidly decrease with VOI size approaching the volume of the target (mouse brain at 0 voxels inflation). Accuracy remains relatively constant with further inflation of the VOI beyond 0 voxels.

4. CONCLUSION

New measures based on union (index *A*) and standard deviation (index *B*) are presented to provide an easy assessment of coregistration accuracy. The strong linearities of the measures are useful in providing insight into the amount of work performed for translating and/or rotating objects during coregistration. These measures are also less volatile to single stray misaligned objects compared to competing intersection-based measures, with index *B* having a better correlation with misregistration than index *A*. With these advantages, different coregistration algorithms may be more effectively compared to each other.

Index *A* and index *B* are not without limitations. One limitation is that the ideal union or ideal standard deviation of a sample needs to be known *a priori*, which are required to set these measures to begin at 0 for perfect alignment. Oftentimes, knowing these in advance may be technically challenging or cumbersome. However, the continued development and improvement of automated segmentation algorithms can greatly aid in this process. Another limitation, specific to index *B*, is its sensitivity to the extent of the background region. Enlarging the encompassing background with empty space, or padding with zeroes, will invariably alter the standard deviation. Ideal accuracy measures should be insensitive to the number of time points, thus care must be taken to keep the extent of the background region as consistent as possible across multiple time points in order to maintain robustness. Additionally, these simulations were performed with line segments along one dimension and further validation will be needed using randomly aligned 3D objects in order to derive a more robust standard deviation measure to be invariant across different DCE-MRI protocols.

Inflation of the target VOI improves coregistration accuracy. However, this improvement is marginal beyond the approximate volume of the target. A VOI that does not encompass the target will likely be susceptible to large errors in coregistration accuracy. In contrast, a VOI that is overinclusive of the target is marginally more accurate but is also computationally more demanding. Increasing the target VOI allows for more information to be analyzed for greater accuracy at the expense of computational performance. Since processing time for coregistration was found to depend linearly with target VOI size, there is diminishing return in accuracy per second for every voxel of inflation beyond the volume of the target. Additionally, generously inflating the VOI beyond the target may lead to inclusion of erroneous or irrelevant data that may decrease coregistration accuracy. In this study, the brain is a relatively simple case where little exists beyond the calvarium. The brain also comprises the majority of the head, and is clearly defined and stationary relative to surrounding tissues. Therefore, the relatively constant accuracy after 0 voxels inflation is not surprising because the additional amount of data included in incrementally inflating the VOI beyond the brain was a fraction compared to the brain itself. Significant changes in accuracy were not expected with further inflation of the VOI beyond 0 voxels because the amount of data to cause significant misregistration was simply nonexistent with our dataset. Nevertheless, we recommend a conservative approach and including marginally more beyond the volume of the target (5 voxels inflation) to make the most of coregistration accuracy and computational performance.

DCE-MRI of the abdomen presents a more complex situation compared to DCE-MRI of the head with smaller targets in relation to the entire abdomen and a greater degree of surrounding signal, including other abutting organs, which may cause significant misregistration with inflation of the target VOI. Organs in the abdomen, such as the kidney, are also susceptible to movement due to respiration and are not stationary relative to surrounding tissues, making conditions more unpredictable. In addition, isotropic resolution may not be available due to image acquisition technique. Hence, the conclusions drawn from this study may not extend to other organs and further investigation of other organs is warranted. Future work will involve validating the results of this study with 4D coregistration using a serial algorithm as well as more complex voxel similarity measures, such as mutual information, and extending these results suggested by mouse brain DCE-MRI to the clinical setting of human DCE-MRI of the liver, spleen, and kidneys.

REFERENCES

- [1] S. Klein, M. Staring, K. Murphy *et al.*, "elastix: a toolbox for intensity-based medical image registration," *IEEE Trans Med Imaging*, 29(1), 196-205 (2010).
- [2] L. R. Dice, "Measures of the Amount of Ecologic Association Between Species," *Ecology*, 26(3), 297-302 (1945).
- [3] A. Bertrand, U. Khan, D. M. Hoang *et al.*, "Non-invasive, in vivo monitoring of neuronal transport impairment in a mouse model of tauopathy using MEMRI," *Neuroimage*, 64, 693-702 (2013).